Available online at www.sciencedirect.com
ScienceDirect
Trans. Nonferrous Met. Soc. China 22(2012) 803−809
Transactions of Nonferrous Metals Society of China
www.tnmsc.cn

Influence of dual retrogression and re-aging temper on microstructure, strength and exfoliation corrosion behavior of Al−Zn−Mg−Cu alloy

PENG Guo-sheng, CHEN Kang-hua, CHEN Song-yi, FANG Hua-chan

State Key Laboratory for Powder Metallurgy, Central South University, Changsha 410083, China

Received 27 April 2011; accepted 26 July 2011

Abstract: Influence of dual retrogression and re-aging (dual-RRA) temper on microstructure, strength and exfoliation corrosion (EC) behavior of Al−Zn−Mg−Cu alloy was investigated by hardness measurements, tensile properties tests, exfoliation corrosion tests, transmission electron microscopy (TEM) and scanning electron microscopy (SEM) observation combined energy dispersive X-ray detector (EDX) analysis. Dual-RRA temper maintains the matrix precipitates (MPs) similar to RRA temper, meanwhile obtains coarser and sparser grain boundary precipitates (GBPs) as well as higher Cu and lower Zn content compared with T76 temper. Therefore, dual-RRA temper not only keeps strength equivalent to the RRA temper but also obtains higher EC resistance than T76 temper.

Key words: aluminum alloy; retrogression and re-aging; microstructure; tensile properties; exfoliation corrosion

1 Introduction

High strength Al−Zn−Mg−Cu (7000 series) aluminum alloys have been widely used in aircraft structures because of their high strength and low density [1]. The accepted precipitation sequences for 7000 series alloys [2] are as follows: supersaturated solid solution (SSS)→coherent GP zones→semi-coherent intermediate η' ($MgZn_2$) →incoherent stable η($MgZn_2$). These series of alloys provide high strength in the T6 temper but are prone to local corrosion [3]. The over aged temper can effectively improve corrosion resistance with 10%−15% loss of peak strength [4]. RRA temper was developed to improve corrosion resistance with retention of strength [5−9]. The temper involves a short time retrogression applied to the 7000 series aluminum alloy after the T6 temper, followed by water quenching and a final re-aging treatment equivalent to the original T6 temper. Retrogression should be carried out at a temperature below the solvus line of the alloy, but high enough to allow for the partial or complete dissolution of GP zones and fine η' ($MgZn_2$) precipitates. The microstructure resulting from the RRA is fine η' precipitates within the grains similar to the T6 condition and η precipitates distribution at the grain boundaries similar to the T7 temper. The microstructure characterization can improve corrosion resistance without strength loss.

Previous work [10] showed that repetitive-RRA temper could further improve stress corrosion cracking (SCC) resistance without the loss of strength compared with RRA temper. In this work, we emphasized the evolution of microstructure by dual-RRA treatment, trying to find if dual-RRA treatment could improve exfoliation corrosion (EC) resistance without loss of strength, compared with RRA treatment.

2 Experimental

The alloy used in this study was rolled 7B50 plate with a thickness of 20 mm, whose compositions are listed in Table 1.

The specimens were treated by solution (480 °C, 30 min) and cold water quenching, followed by different ageing tempers (see Table 2). Since a very long aging time leads to transforming phase from η' into η, which is difficult to be dissolved during the dual-retrogression, interim-reaging time is 12 h, not 24 h. In addition, T76 and RRA tempers were arranged as reference.

Foundation item: Projects (2010CB731701, 2012CB619502) supported by the National Basic Research Program of China; Project (50721003) supported by the Creative Research Group of National Natural Science Foundation of China
Corresponding author: CHEN Kang-hua; Tel: +86-731-88830714; Fax: +86-731-88710855; E-mail: khchen@mail.csu.edu.cn
DOI: 10.1016/S1003-6326(11)61248-X

Table 1 Nominal composition of 7B50 alloy (mass fraction, %)

Zn	Mg	Cu	Zr	Al
6.5	2.4	2.2	0.15	Bal.

Table 2 Aging treatments applied to 7B50 alloy

Aging treatment	1st step	2nd step	3rd step	4th step	5th step
T76	120 °C, 6 h	160 °C, 12 h	–	–	–
RRA	120 °C, 24 h	180 °C, 30 min	120 °C, 24 h	–	–
Dual-RRA	120 °C, 24 h	180 °C, 30 min	120 °C, 12 h	180 °C, 5−60 min	120 °C, 24 h

The hardness has been evaluated by Vickers hardness tests. The hardness values reported here represent the average of at least five measurements. Electrical conductivity was determined using an SX1931 digital micrometer. The tensile tests were performed by a CSS−44100 testing machine at RT, using smooth plate specimens. Transmission electron microscope (JEOL 2100−F) was used to observe typical microstructures, among which grain boundary precipitates (GBPs) observation focused on high angle grain boundary. Energy dispersive X-ray detector (EDX) was used to identify the content of GBPs. Since Al matrix may be involved in the EDX signal of GBPs, the values obtained from EDX analysis only reflect the content change tendency. Specimens for all TEM observations were taken from the $T/2$ positions in the plate (T is plate thickness) perpendicular to the rolling direction and electro-polished in a solution of 25% HNO_3 in methanol at −45 °C and 15 V. The accelerated exfoliation corrosion test was performed at room temperature according to the exfoliation corrosion(EXCO) test as described in ASTM G34 — 79 [11]. The EXCO solution of 4.0 mol/L NaCl+0.5 mol/L KNO_3+ 0.1 mol/L HNO_3 (pH=0.4) was used. After 48 h of continuous immersion in the EXCO solution, the sample corrosion morphology was recorded by a digital camera and optical micrography.

3 Results

3.1 Determination of dual-retrogression time in dual-RRA treatment

Typical morphologies of samples with different dual-retrogression time at 180 °C are shown in Fig. 1.

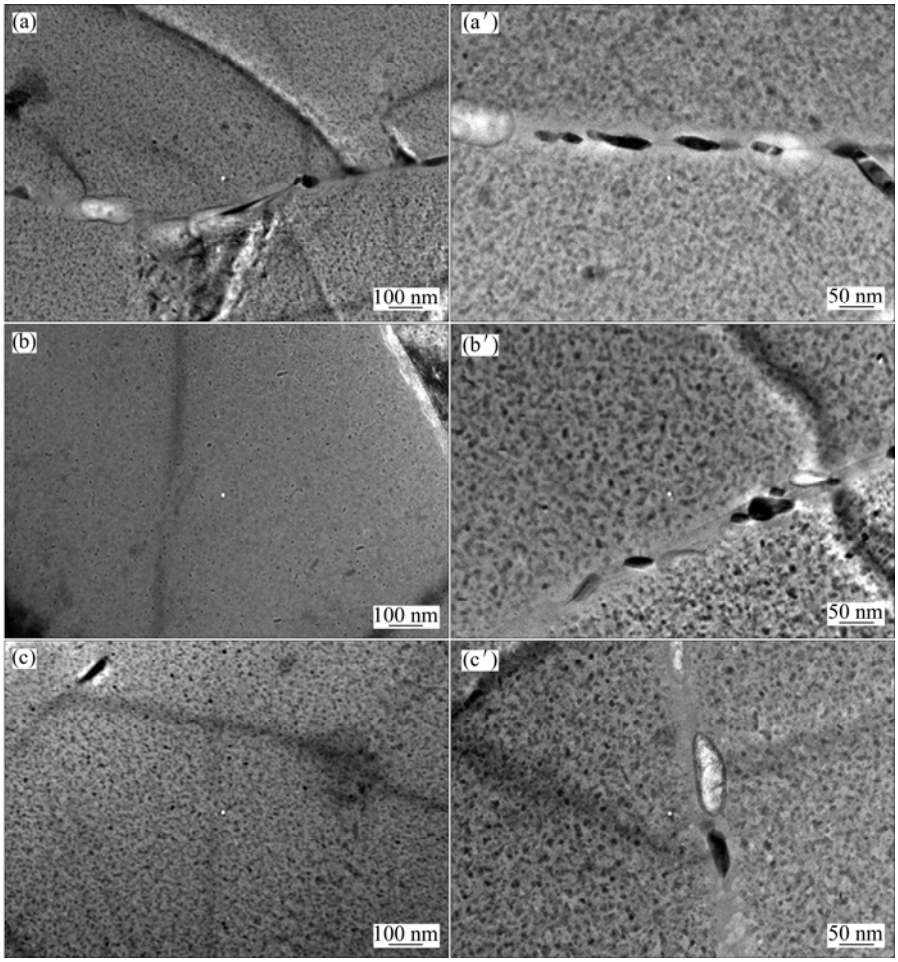

Fig. 1 Evolution of microstructure of 7B50 Al alloy with different dual-retrogression time: (a), (a′) 5 min; (b), (b′) 30 min; (c), (c′) 60 min

It can be seen that MPs experience dissolution and coarsening process with dual-retrogression time increasing. When the dual-retrogression time is within 30 min, small MPs completely dissolve, only leaving few large MPs undissolved. Further elongating the dual-retrogression time, MPs and GBPs grow coarser.

The corresponding diffraction patterns with different dual-retrogression time are shown in Fig. 2. When dual-retrogression time is 5 min, weak diffraction spots at {1, (2n+1)/4, 0} positions in Al $\langle\bar{1}22\rangle$ projection, which are corresponding to the diffraction features of GP zones [10], can be observed. In addition, a diffraction feature corresponding to η' particles can be clearly identified, such as weak diffraction spots at 1/3 and 2/3 of {4 2 0} in Fig. 2(a). This indicates that GP zones and η' particles predominate MPs at the dual-retrogression initial stage. After 30 min of dual-retrogression time, GP diffraction spots disappear and a pair of spots which are very close to 2/3 of {4 2 0} position in Al $\langle\bar{2}33\rangle$ projection appear, as shown in Fig. 2(b), indicating that η phases have already formed. It agrees with the observation of SHA and CEREZO [12].

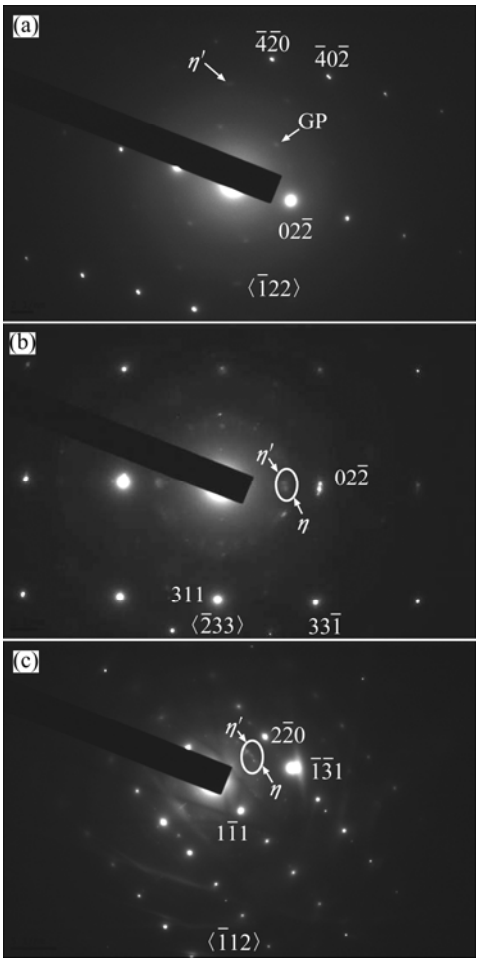

Fig. 2 Corresponding diffraction patterns of 7B50 alloy with different dual-retrogression time: (a) 5 min; (b) 30 min; (c) 60 min

Further prolonging dual-retrogression time, diffraction spots of η' and η particles become slightly stronger, as shown in Fig. 2(c). This suggests that the volume fraction of η' and η phases increases.

The influences of dual-retrogression time on dual-RRA hardness and conductivity are summarized in Fig. 3. The hardness values reported here represent the average of at least five measurements. It is obvious that the highest hardness is obtained when dual-retrogression time is 30 min, so the proper dual-retrogression condition is 180 °C, 30 min. The conductivity increases with the prolonging dual-retrogression time because precipitates get coarse.

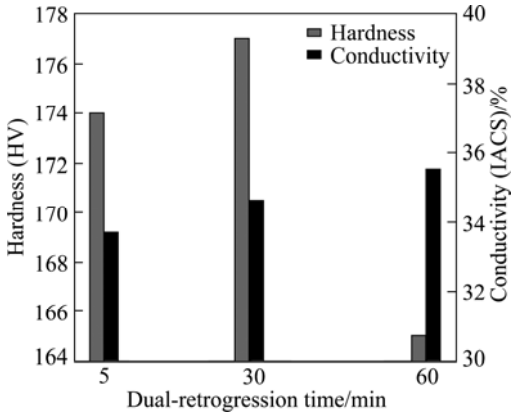

Fig. 3 Effect of dual-retrogression time on hardness and conductivity

3.2 Effects of dual-RRA on microstructure and strength

The microstructures of 7B50 Al alloy by RRA, dual-RRA and T76 tempers, respectively, are shown in Fig. 4. Compared with RRA temper, the MPs size by dual-RRA temper is similar, but its size is smaller than that by T76 temper. The corresponding diffraction patterns of different aging tempers are shown in Fig. 5. The diffraction patterns of dual-RRA are similar to those of RRA and the corresponding η' and η phases are weaker than those of T76. It is interesting that dual-RRA temper has a remarkable effect on the GBPs, the GBPs grow coarser and sparser than those by RRA temper, slightly coarser and sparser compared with those by T76.

In addition, the GBP compositions of samples by different aging tempers are shown in Fig. 6. Obviously, the Cu content of GBPs by dual-RRA temper is higher than that by RRA temper, and T76 temper, inversely for Zn content.

The tensile properties for 7B50 Al alloy treated by different aging tempers are listed in Table 3. The strength by dual-RRA is similar to that by RRA. The ultimate tensile strength (UTS) is about 610 MPa, and yield strength (YS) is about 585 MPa, which are greater than

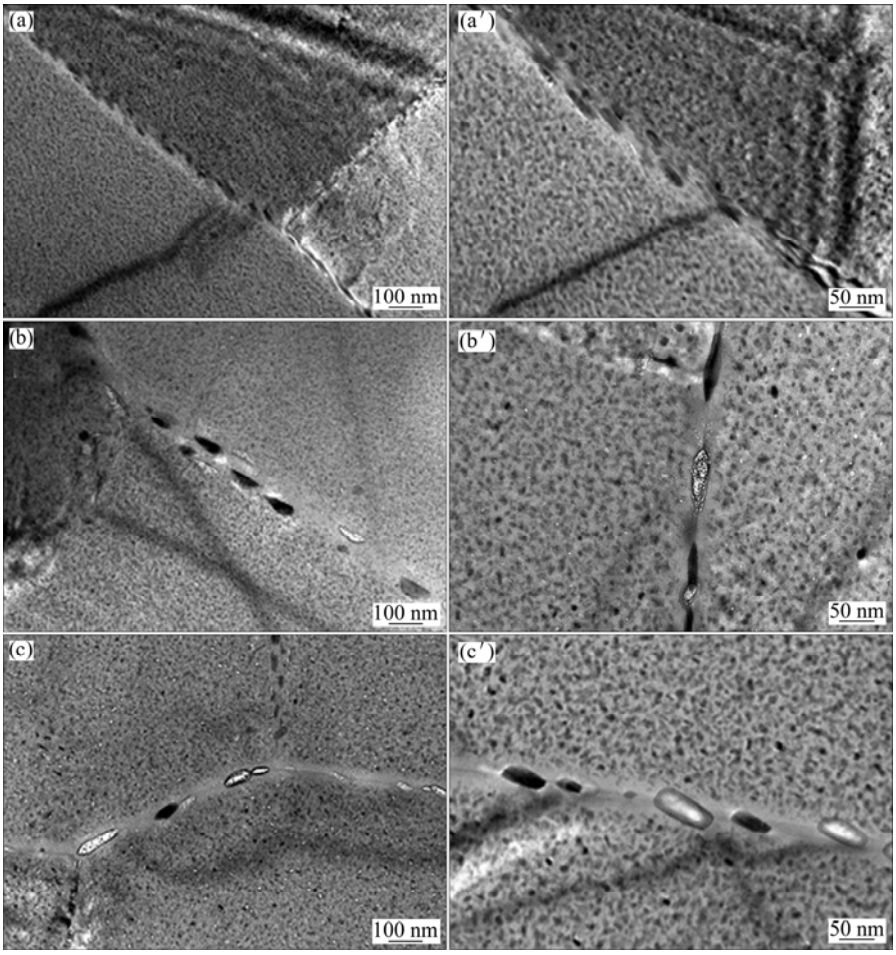

Fig. 4 Microstructures of 7B50 Al alloy by different aging tempers: (a), (a′) RRA; (b), (b′) Dual-RRA; (c), (c′) T76

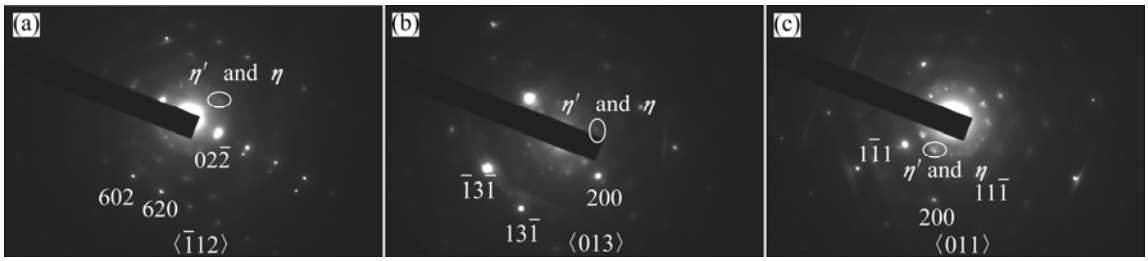

Fig. 5 Corresponding diffraction patterns of 7B50 alloy by different aging tempers: (a) RRA; (b) Dual-RRA; (c) T76

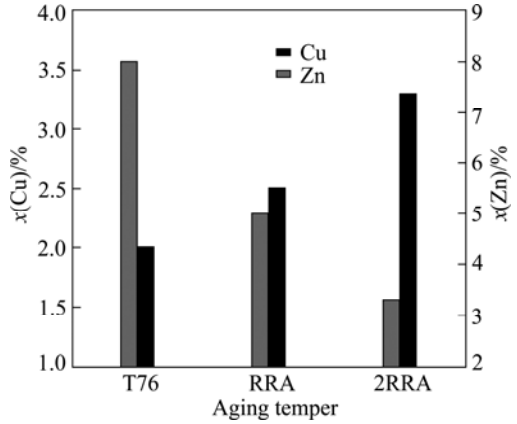

Fig. 6 Copper and zinc element content in grain boundary precipitates for 7B50 alloy treated by different aging tempers

Table 3 Conductivity and tensile properties for 7B50 alloy treated by different aging treatments

Aging temper	UTS/MPa	YS/MPa	EI/%
T76	556.3	525.5	12.4
RRA	612.4	585.2	13.6
Dual-RRA	611.5	585.5	13.9

those by T76 (about 556 MPa UTS and 525 MPa YS). The elongation (EI) slightly increases compared with RRA. Fracture surfaces also indicate that the samples by dual-RRA and RRA tempers have higher strength than that by T76 (see Fig. 7). Fracture surfaces by dual-RRA and RRA temper exhibit more uneven surfaces and

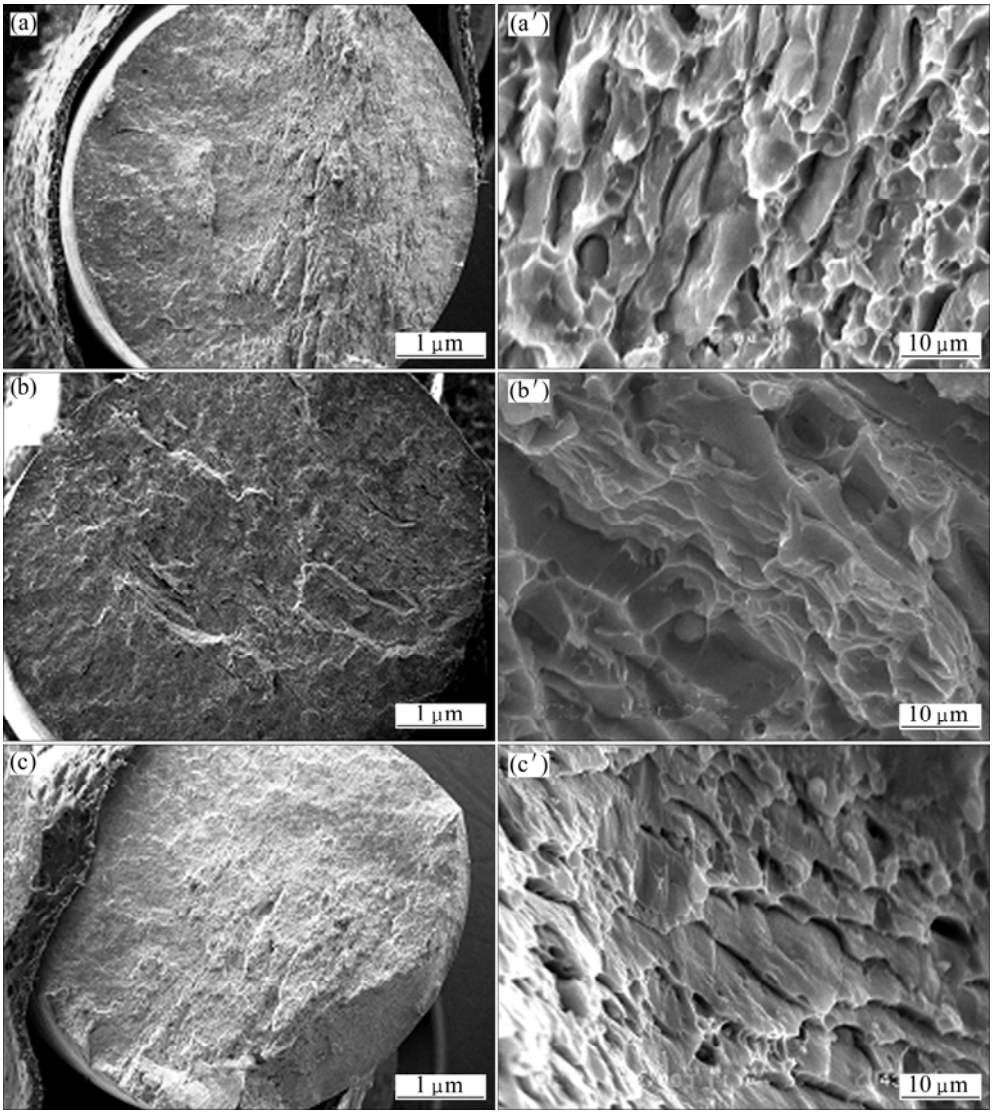

Fig. 7 Fracture surface of 7B50 alloy by different aging tempers: (a), (a′) RRA; (b), (b′) Dual-RRA; (c), (c′) T76

deeper ductile dimples by low and high magnification, respectively.

3.3 Effects of dual-RRA on EC

The EC morphologies of the 7B50 alloy by various aging tempers are shown in Fig. 8.

EC rate can be summarized by the EXCO rate standard: E_D(=Severe exfoliation)>E_C>E_B>E_A>P (=Slight amount of incipient exfoliation), where P represents pitting corrosion and E_A−E_D describe a range from superficial to severe exfloliation. Figure 8(a) presents the corrosion morphology of alloy by RRA. Clearly, multi-surface layers are peeled off and deeper etch pits are observed with corrosion rating E_C. As a comparison, the corrosion morphology of alloy by dual-RRA only shows part separation of metal occurs (rating: E_A, Fig. 8(b)). Figure 8(c) exhibits the corrosion morphology of alloy by T76. The whole superficial exfoliation surface occurs and only a small number of tiny blisters are observed, which is rated by E_B. Therefore, the EC resistance is the order of RRA<T76<dual-RRA.

4 Discussion

It is well acknowledged [7] that the main microstructural changes during retrogression and re-aging are the partial dissolution of GP zones and fine η' precipitates in the matrix and re-precipitated during the re-aging, while η($MgZn_2$) precipitates at the grain boundaries are allowed to form and coarse. Therefore, it can be speculated that proper dual-RRA temper will obtain MPs similar to that by RRA temper, while GBPs grow coarser and sparser compared with those of T76 temper. The TEM microstructure observation testified the assumption. Dual-RRA temper obtains the MPs size which is similar to that of RRA and smaller than T76. The corresponding diffraction patterns show that the MPs of RRA, dual-RRA and T76 mainly consist of η'

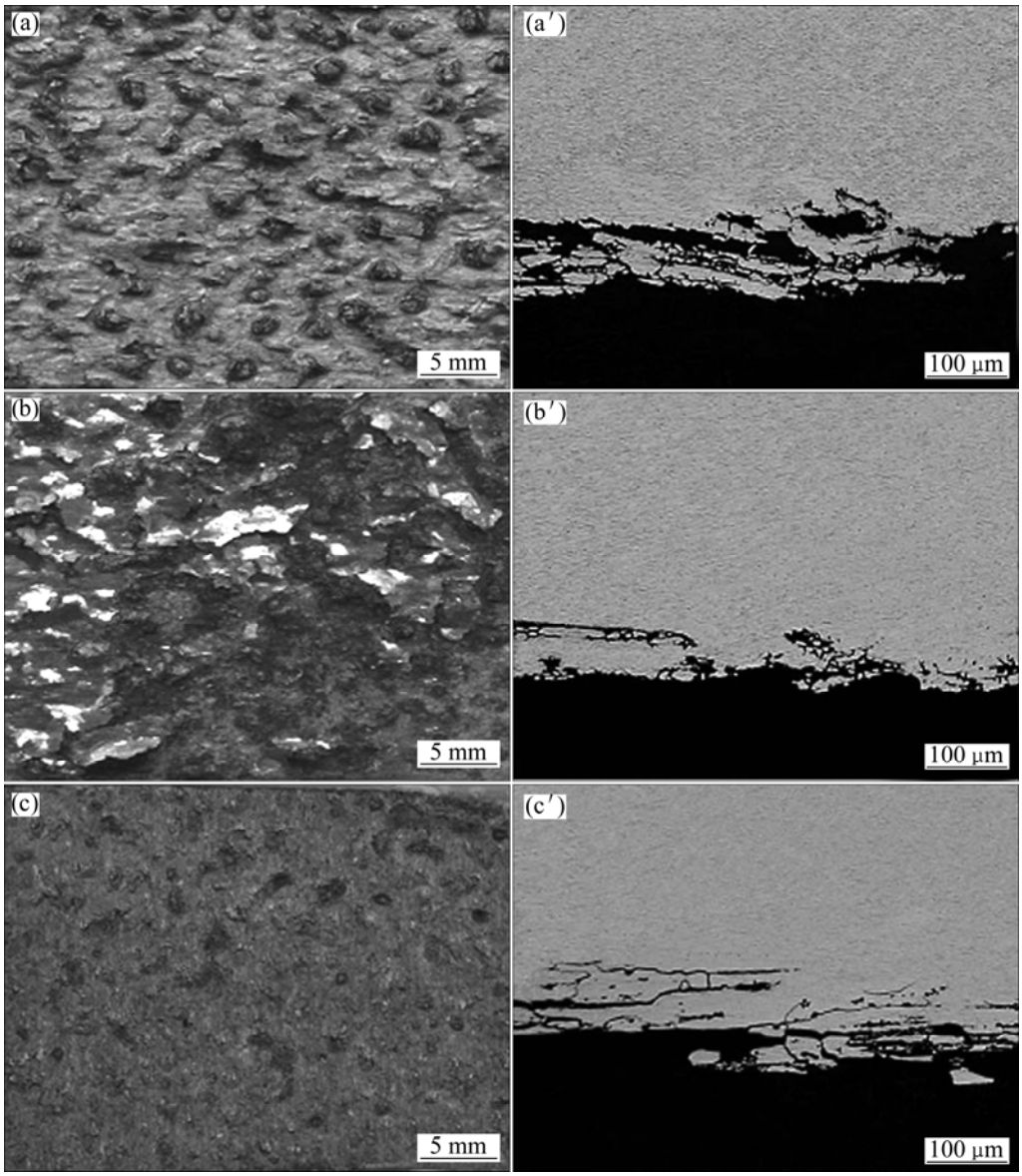

Fig. 8 EC morphologies of 7B50 alloy by different aging tempers: (a), (a′) RRA; (b), (b′) Dual-RRA; (c), (c′) T76 (EC surfaces (c) and cross-section (c′))

and η phases. However, the diffraction patterns of T76 are stronger compared with RRA and dual-RRA, suggesting that η' and η phases become coarser. The reason contributes to η' and η phases coarsening, which agrees with the TEM observation and the loss of strength. Since EC is a form of intergranular corrosion [13,14], EC is associated with GBPs. The coarser and sparser the GBPs are, the lower the intergranular corrosion rate is, the higher the EC resistance is. In addition, the high Cu content of GBPs decreases the galvanic interaction between GBPs and adjacent matrix [15,16], inhibiting intergranular corrosion initiation and improving the EC resistance. So, the coarse and sparse GBPs along with higher Cu content of GBPs by dual-RRA remarkably improve EC resistance.

5 Conclusions

1) Under the condition of RRA (120 °C, 24 h+180 °C, 30 min+120 °C, 12 h), proper dual-retrogression condition is 180 °C, 30 min for 7B50 Al alloy studied, which leads to small MPs dissolving.

2) Dual-RRA temper can maintain MP size similar to RRA temper, meanwhile obtain coarser and sparser GBPs than T76 temper.

3) Dual-RRA temper not only keeps strength equivalent to the RRA temper but also obtains higher EC resistance than T76 temper.

4) The higher EC resistance by dual-RRA contributes to coarser and sparer distribution as well as

higher Cu and lower Zn content of GBPs compared with T76 temper.

References

[1] HEINZ A, HASZLER A, KEIDEL C, MOLDENHAUER S, BENEDICTUS R, MILLER W S. Recent development in aluminium alloys for aerospace applications [J]. Mater Sci Eng A, 2000, 280(1): 102−107.

[2] DEGISCHER H P, LACOM W, ZAHRA A, ZAHRA C Y. Decomposition process in an Al-5% Zn-1% Mg alloy [J]. Metallk Z, 1980, 71(1): 231−238.

[3] SPEIDEL M O. Stress corrosion cracking of aluminum alloys [J]. Metall Trans A, 1975, 6(4): 631−642.

[4] XIONG Bai-qing, LI Xi-wu, ZHANG Yong-an, LI Zhi-hui, ZHU Bao-hong, WANG Feng, LIU Hong-wei. Novel Al−7.5Zn−1.65Mg−1.4Cu−0.12Zr alloys with high strength, high toughness and low quench sensitivity [J]. Transactions of Nonferrous Metals Society of China, 2009, 19(9): 1539−1547.

[5] MENG C F, LONG H W, ZHENG Y. A study of the mechanism of hardness change of Al−Zn−Mg Alloy during retrogression reaging tempers by small angle X-ray scattering (SAXS) [J]. Metall Mater Trans A, 1997, 28(10): 2067−2071.

[6] DANH N C, RAJAN K, WALLACE W. A TEM study of microstructural changes during retrogression and reaging in 7075 aluminum [J]. Metall Trans A, 1983, 14(9): 1843−1850.

[7] NING Ai-lin, LIU Zhi-yi, PENG Bei-shan, ZENG Su-min. Redistribution and re-precipitation of solute atom during retrogression and reaging of Al−Zn−Mg−Cu [J]. Transactions of Nonferrous Metals Society of China, 2007, 17(5): 1005−1011.

[8] PARK J K, ARDELL A J. Effect of retrogression and reaging tempers on the microstructure of Al-7075-T651 [J]. Metall Trans A, 1984, 15(8): 1531−1543.

[9] FENG Chun, LIU Zhi-yi, NING Ai-ling, ZENG Su-ming. Retrogression and re-aging temper of A1−9.99Zn−1.72%Cu−2.5%Mg−0.13%Zr aluminum alloy [J]. Transactions of Nonferrous Metals Society of China, 2006, 16(5): 1163−1170.

[10] PENG Guo-sheng, CHEN Kang-hua, CHEN Song-yi, FANG Hua-chan. Influence of repetitious-RRA treatment on the strength and SCC resistance of Al−Zn−Mg−Cu alloy [J]. Mater Sci Eng A, 2011, 528(12): 4014−4018.

[11] ASTM G34—79. Standard Test method for exfoliation corrosion susceptibity in 2xxx and 7xxx Series Aluminum Alloys (EXCO test) [S].

[12] SHA G, CEREZO A. Early-stage precipitation in Al−Zn−Mg−Cu alloy (7050) [J]. Acta Mater, 2004, 52(15): 4503−4516.

[13] MCNAUGHTAN D, WORSFOLD M, ROBINSON M J. Corrosion product force measurements in the study of exfoliation and stress corrosion cracking in high strength aluminium alloys [J]. Corr Sci, 2003, 45(10): 2377−2389.

[14] ROBINSON M J, JACKSON N C. The influence of grain structure and intergranular corrosion rate on exfoliation and stress corrosion cracking of high strength Al−Cu−Mg alloys [J]. Corr Sci, 1999, 41(5): 1013−1028.

[15] KNIGHT S P, BIRBILIS N, MUDDLE B C, TRUEMAN A R, LYNCH S P. Correlations between intergranular stress corrosion cracking, rain-boundary microchemistry and grain-boundary electrochemistry for Al–Zn–Mg–Cu alloys [J]. Corr Sci, 2010, 52(12): 4073−4080.

[16] RAMGOPAL T, GOUMA P I, FRANKEL G S. Role of grain-boundary precipitates and solute-depleted zone on the intergranular corrosion of aluminum alloy 7150 [J]. Corrosion, 2002, 58(8): 687−697.

二次回归再时效对 Al−Zn−Mg−Cu 组织、强度及剥蚀性能的影响

彭国胜，陈康华，陈送义，方华婵

中南大学 粉末冶金国家重点实验室，长沙 410083

摘　要：采用硬度、拉伸和剥落腐蚀测试手段，结合透射电镜和扫描电镜观察以及能谱分析，研究二次回归再时效对组织、力学和剥蚀性能的影响。二次回归再时效处理保持了类似一次回归再时效处理的晶内析出相，得到比 T76 过时效更粗大且离散的晶界析出相。与 T76 相比，二次回归再时效处理的晶界析出相具有更高的铜含量和更低的锌含量。因此，二次回归再时效处理保持了一次回归再时效处理的强度，同时得到了比 T76 过时效处理更高的剥蚀抗力。

关键词：铝合金；回归再时效(RRA)；微观组织；拉伸性能；剥落腐蚀

(Edited by LI Xiang-qun)